ACOUSTIC SCATTERING FROM A TURBULENT VORTEX

Vernon W. Ramsey, et al

Stanford University

Prepared for:

Office of Naval Research
National Aeronautics and Space Administration

January 1974

SECURITY CLASSIFICATION OF THIS PAGE (When Data Entered)

AD786 687

REPORT DOCUMENTATION PAGE

READ INSTRUCTIONS BEFORE COMPLETING FORM

1. REPORT NUMBER: SU-SEL-74-001
2. GOVT ACCESSION NO.
3. RECIPIENT'S CATALOG NUMBER

4. TITLE (and Subtitle)

ACOUSTIC SCATTERING FROM A TURBULENT VORTEX

5. TYPE OF REPORT & PERIOD COVERED: Interim

6. PERFORMING ORG. REPORT NUMBER: 3606-9

7. AUTHOR(s)

Vernon W. Ramsey and Allen M. Peterson
Center for Radar Astronomy
Stanford University
Stanford, California 94305

8. CONTRACT OR GRANT NUMBER(s)
N00014-67-A-0112-0044
NGL-05-020-014

9. PERFORMING ORGANIZATION NAME AND ADDRESS

Center for Radar Astronomy
Stanford Electronics Laboratories
Stanford University
Stanford, California 94305

10. PROGRAM ELEMENT, PROJECT, TASK AREA & WORK UNIT NUMBERS

12. REPORT DATE: January 1974

13. NO. OF PAGES: ~~27~~ 34

11. CONTROLLING OFFICE NAME AND ADDRESS

Stanford Electronics Laboratories, Director
Stanford University
Stanford, California 94305

15. SECURITY CLASS. (of this report): Unclassified

14. MONITORING AGENCY NAME & ADDRESS (if diff. from Controlling Office)

15a. DECLASSIFICATION/DOWNGRADING SCHEDULE

16. DISTRIBUTION STATEMENT (of this report)

This document has been approved for public use and sale; its distribution is unlimited.

17. DISTRIBUTION STATEMENT (of the abstract entered in Block 20, if different from report)

18. SUPPLEMENTARY NOTES

19. KEY WORDS (Continue on reverse side if necessary and identify by block number)

Acoustics
Scattering
Trailing Vortex
Turbulence
Spectral Density

20. ABSTRACT (Continue on reverse side if necessary and identify by block number)

With the aid of the Born approximation, the time autocorrelation and power spectral density are calculated for the received acoustic signal scattered from velocity fluctuations in a turbulent aircraft trailing vortex. The turbulence is required to be globally stationary, but only locally homogeneous. The treatment includes the effects of spectral broadening due to convection of the scattering eddies by a spatially varying mean flow and by macroeddies. The 3 dB bandwidth of the received signal is related to the scattering angle and the core Mach number of the vortex. A primary feature of the analysis is that it provides a method

DD FORM 1 JAN 73 1473
EDITION OF 1 NOV 65 IS OBSOLETE

SECURITY CLASSIFICATION OF THIS PAGE (When Data Entered)

19 KEY WORDS (Continued)

20 ABSTRACT (Continued)

for inferring the radial intensity distribution of turbulence in a vortex. The analysis technique is also applicable to scattering from other turbulent flows where significant variations of turbulence level occur over distances on the order of the macroeddy size.

ACOUSTIC SCATTERING FROM A TURBULENT VORTEX

by

Vernon W. Ramsey*

and

Allen M. Peterson

January 1974

Technical Report 3606-9

Work supported by

Joint Services Electronics Programs
Under Office of Naval Research
Contract N00014-67-A-0112-0044

and by

National Aeronautics and Space Administration
Under Grant NGL 05-020-014

*Hughes Aircraft Company, Fullerton, California

Radioscience Laboratory
Stanford Electronics Laboratories
Stanford University Stanford, California

ABSTRACT

With the aid of the Born approximation, the time autocorrelation and power spectral density are calculated for the received acoustic signal scattered from velocity fluctuations in a turbulent aircraft trailing vortex. The turbulence is required to be globally stationary, but only locally homogeneous. The treatment includes the effects of spectral broadening due to convection of the scattering eddies by a spatially varying mean flow and by macroeddies. The 3 dB bandwidth of the received signal is related to the scattering angle and the core Mach number of the vortex. A primary feature of the analysis is that it provides a method for inferring the radial intensity distribution of turbulence in a vortex. The analysis technique is also applicable to scattering from other turbulent flows where significant variations of turbulence level occur over distances on the order of the macroeddy size.

CONTENTS

ILLUSTRATIONS

I. INTRODUCTION

The detection of aircraft trailing vortices by acoustic scattering has in recent years been developed to the status of a practical experimental technique. Of notable significance in this area is the work reported by Balser, Nagy, and Proudian.[1] The pioneering efforts of this group have also demonstrated the potential usefulness of acoustic scattering as a tool for studying the detailed *structure* of turbulent vortices. The study of vortex structure by acoustic methods is the theme to which this paper is addressed.

The problem to be considered is that of three-dimensional scattering from a finite section of a single turbulent vortex. The treatment utilizes two theories developed by R. A. Silverman: one his theory of local homogeneity,[2] and the other his model for calculating spectral broadening due to macroeddies.[3] The macroeddy model has been applied to scattering from globally homogeneous turbulence (as distinguished from *locally* homogeneous turbulence) by Ford and Meecham.[4] While the restriction to global homogeneity should be acceptable for describing scattering from large volumes of atmospheric turbulence, the resulting theories are probably not as useful for predicting signal spectra from aircraft vortices and other turbulent flows where the intensity of turbulence varies rapidly over distances of a few macroeddies.

II. MEAN VELOCITY DISTRIBUTION

It will be evident later on that the correlation time of the received

scattered signal is exceedingly small in comparison to observed time scales of decay of actual aircraft vortices, which are typically a full minute or more. Let us therefore imagine the vortex velocity $\underset{\sim}{v}(\underset{\sim}{r},t)$ being time-averaged over an interval which is very long in comparison to the signal correlation time, but very short in comparison to the vortex decay time. Denoting this averaging operation by angular brackets, we wish to model the result so obtained by the sum

$$\left\langle \underset{\sim}{v}(\underset{\sim}{r},t) \right\rangle = \underset{\sim}{u}_0 + \underset{\sim}{V}(\underset{\sim}{r}) \tag{1}$$

The spatially varying component $\underset{\sim}{V}(\underset{\sim}{r})$ represents the mean swirl velocity, and will be discussed presently. The constant vector $\underset{\sim}{u}_0$ will represent the combined effects of wind and drift in moving the entire vortex as a unit. Using (1), we then express the overall velocity field in the form

$$\underset{\sim}{v}(\underset{\sim}{r},t) = \underset{\sim}{u}_0 + \underset{\sim}{V}(\underset{\sim}{r}) + \underset{\sim}{u}(\underset{\sim}{r},t) \tag{2}$$

where $\underset{\sim}{u}(\underset{\sim}{r},t)$ is the fluctuation of $\underset{\sim}{v}(\underset{\sim}{r},t)$ about its mean value.

The swirl velocity $\underset{\sim}{V}(\underset{\sim}{r})$ in (1) will be assumed to be a truncated two-dimensional flow having radial symmetry about the z axis in Fig. 1. It will be taken to be entirely circumferential with no radial or axial components. Measurements[5] have shown that the magnitude of $\underset{\sim}{V}(\underset{\sim}{r})$ increases almost linearly from zero at the center to its maximum value, and then diminishes more slowly toward zero with radial distance from the vortex axis. The maximum velocity attained is commonly called the *core velocity*, which we will denote by V_c. The radial distance from the axis at which this peak velocity occurs, called the *core radius*, will be denoted by r_c. The central region of radius r_c is called the *core* of the vortex.

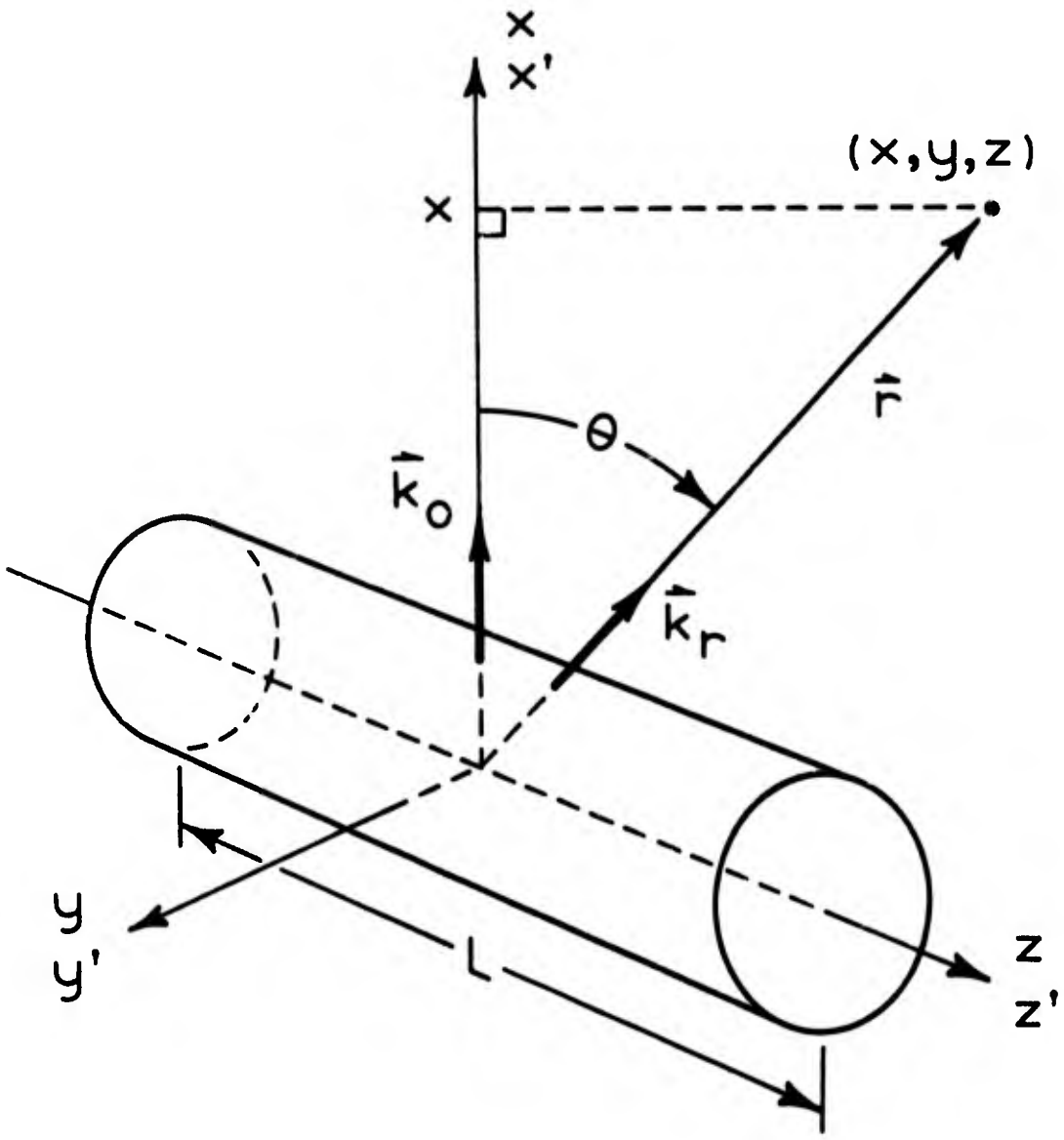

Figure 1. VORTEX COORDINATE SYSTEM

The two-dimensional character of $\underset{\sim}{V}(\underset{\sim}{r})$ might be emphasized by writing its magnitude as $V(\sigma)$, where σ is the perpendicular distance from the z axis of Fig. 1. For illustrating the theory, we shall use a radial distribution of circumferential velocity having a magnitude defined by

$$V(\sigma) = V_c f(\sigma) \tag{3}$$

where $f(\sigma)$ is a dimensionless distribution given by

$$f(\sigma) = A r_c \sigma^{-1} [1 - \exp(-\chi \sigma^2 / r_c^2)] \tag{4}$$

Definitions (3) and (4) represent a laminar-flow solution obtained originally by Lamb,[6] and recast here in a form similar to that used by Georges[7] and others. From the definitions of V_c and r_c above, it is seen from (3) that $f(\sigma)$ must attain a peak value of unity, and that this peak must occur at $\sigma = r_c$. The approximate values of A and χ satisfying these conditions are $A = 1.398$ and $\chi = 1.256$. A plot of $f(\sigma)$ with the argument normalized to r_c is shown in Fig. 1 of Georges' paper.[7]

It will also be useful to define a vortex core Mach number by

$$M = V_c/c \tag{5}$$

where c is the isentropic sonic velocity in the undisturbed medium, i.e., in the absence of a vortex or turbulence. Even in the largest present-day aircraft, the core Mach numbers seldom exceed 0.2. Since the macroscale velocity for turbulence in an aircraft vortex should be roughly equal to the core velocity, the low Mach numbers involved justify a neglect of compressibility effects with respect to all but sound wave fluctuations.

III. SCATTERING EQUATION

The scattering configuration is shown in Fig. 1. A uniform plane wave is assumed to be incident from below, illuminating a vortex section of length L centered about the coordinate origin. The effect of a finite antenna beamwidth is taken care of by truncating the vortex.

Neglecting scattering from temperature fluctuations, assuming incompressibility of the flow field, and considering only incident acoustic frequencies which are very high in comparison to frequencies associated with the turbulence, several authors have correctly derived scattering equations from the basic fluid dynamics equations. Of these derivations, the one by Lighthill,[8] which employs the Born (single-scattering) approximation, is particularly well suited to the present analysis. Using Eqs. 6, 7, and 10 from his paper, contracting the tensor indices, and introducing a few changes of notation, we have the far-zone expression

$$\rho(\underset{\sim}{r},t) = -k_o^2 \times (\tfrac{1}{2}\rho_o c I_i)^{\frac{1}{2}} \pi^{-1} (r c)^{-3}$$

$$\times \int \cos(\omega_o t - k_o x' - k_o R') \; \underset{\sim}{r} \cdot \underset{\sim}{v}(\underset{\sim}{r}', t - R'/c) \; d^3\underset{\sim}{r}' \qquad (6)$$

In (6), $\rho(\underset{\sim}{r},t)$ is the deviation from the ambient density ρ_o due to the sound wave, replacing the difference $(\rho - \rho_o)$ used by Lighthill. The vectors $\underset{\sim}{r}$ and $\underset{\sim}{r}'$ replace Lighthill's $\underset{\sim}{x}$ and $\underset{\sim}{y}$, respectively — the unprimed vector locating field observation points, and the primed vector locating source points. The vector $\underset{\sim}{r}$ is shown in Fig. 1. The distance R' in (6) is the magnitude of the difference vector $(\underset{\sim}{r} - \underset{\sim}{r}')$, and the distance r is

the magnitude of the vector $\underset{\sim}{r}$. The derivation of (6) incorporated an incident cosine plane wave having radian frequency ω_o, wave number $k_o = \omega_o/c$, and propagating in the positive x direction as indicated by the wave vector $\underset{\sim}{k}_o$ in Fig. 1. The intensity of this wave, denoted by I_i in (6), is given by Eq. 7 of Lighthill's paper.

The velocity $\underset{\sim}{v}$ in (6) replaces the velocity fluctuation $\underset{\sim}{v}'$ in Lighthill's Eq. 10. Although Lighthill dealt only with turbulent fluctuations about the mean flow, it is important to note from his derivation that the restriction of $\underset{\sim}{v}$ in (6) to representing only *fluctuations* is not necessary for the validity of the expression.

For the present application, the most appropriate substitution for $\underset{\sim}{v}$ in (6) would be the velocity sum in (2). Retention of the translational velocity $\underset{\sim}{u}_o$ in (2) would cause a pronounced increase in complication, however. Among other things, for sufficiently large values of $\underset{\sim}{u}_o$, the time variation of the scattering angle θ in Fig. 1 would not be negligible. Previous analyses[4,8] have shown that scattering at different angles arises from turbulent eddies of different sizes — which tend to be uncorrelated. The signal correlation time from a vortex sweeping by overhead would consequently be less than that obtained from a nontranslating vortex; or in terms of the power spectral density, a broader spectrum would be recorded.

Even when the velocity $\underset{\sim}{u}_o$ is small enough to neglect the time variation of θ in Fig. 1, the power spectrum would be shifted by an amount corresponding to the ordinary Doppler shift from a moving target. This latter effect is easily taken into account, however, in an analysis which

otherwise neglects $\underset{\sim}{u}_0$. Our procedure here will be to substitute (2) into (6) with $\underset{\sim}{u}_0 = 0$, and then to reinsert $\underset{\sim}{u}_0$ at an appropriate point later on. Since observed values of $\underset{\sim}{u}_0$ in the absence of wind transport seldom exceed 1 or 2 m/sec in magnitude, this procedure should be quite adequate for including the vortex drift effect.

We now must form the lagged mean product $\left\langle \rho(\underset{\sim}{r},t)\ \rho(\underset{\sim}{r},\ t-\tau) \right\rangle$. As the steps involved in going from (6) to this product are documented in Refs. 4, 8, and elsewhere, we simply write down the result and point out the minor differences entailed by the present setup. Substituting (2) into (6), neglecting $\underset{\sim}{u}_0$ in accordance with the argument above, and noting that $\left\langle \underset{\sim}{u}(\underset{\sim}{r},t) \right\rangle = 0$, we construct the product

$$\left\langle \rho(\underset{\sim}{r},t)\ \rho(\underset{\sim}{r},\ t-\tau) \right\rangle = \rho_0 I_i k_0^4 (2\pi r)^{-2} c^{-r} \cos^2\theta$$

$$\times \left\{ \iint V_r(\underset{\sim}{r}')\ V_r(\underset{\sim}{r}'') \cos(\omega_0\tau - \underset{\sim}{k}\cdot\underset{\sim}{\xi})\ d^3\underset{\sim}{r}'\ d^3\underset{\sim}{r}'' \right.$$

$$\left. + \iint \left\langle u_r(\underset{\sim}{r}',t')\ u_r(\underset{\sim}{r}'',t'') \right\rangle \cos(\omega_0\tau - \underset{\sim}{k}\cdot\underset{\sim}{\xi})\ d^3\underset{\sim}{r}'\ d^3\underset{\sim}{r}'' \right\} \qquad (7)$$

where

$$\underset{\sim}{\xi} = \underset{\sim}{r}'' - \underset{\sim}{r}' \qquad (8)$$

$$\underset{\sim}{k} = \underset{\sim}{k}_0 - \underset{\sim}{k}_r \qquad (9)$$

$$t' = t - \tau - R'/c \qquad (10)$$

$$t'' = t - R''/c \qquad (11)$$

and where $R' = |\underset{\sim}{r} - \underset{\sim}{r}'|$ and $R'' = |\underset{\sim}{r} - \underset{\sim}{r}''|$. The r component $V_r(\underset{\sim}{r}')$ results from evaluating the dot product in (6) involving the unit vector $\underset{\sim}{r}/r$, and

similarly for $u_r(\underset{\sim}{r}',t)$. The scattering vector $\underset{\sim}{k}$ in (9) is constructed from the two wave vectors shown in Fig. 1. These two vectors have equal magnitudes, $|k_o| = |k_r| = k_o = \omega_o/c$, and as a result, $\underset{\sim}{k}$ has the magnitude

$$k = |\underset{\sim}{k}| = 2\, k_o \sin(\tfrac{1}{2}\theta) \tag{12}$$

Since the coordinate x in (6) is the x component of the position vector $\underset{\sim}{r}$, we note from Fig. 1 that $x/r = \cos\theta$. This substitution has also been included in (7).

With the mean vortex flow included, we have obtained two scattering integrals instead of one. The first integral in (7) represents scattering from the frozen-in refractive index field created by the mean flow, and has been subjected to various two-dimensional[9-11] and three-dimensional[12] treatments. The corresponding power spectral density, defined from the Wiener-Kintchine relationship by

$$P(\underset{\sim}{r},\omega) = (2\pi c_o I_i)^{-1} c^2 \int_{-\infty}^{\infty} \left\langle \rho(\underset{\sim}{r},t)\, \rho(\underset{\sim}{r},\, t-\tau) \right\rangle e^{-i\omega\tau}\, d\tau \tag{13}$$

is easily shown to be a line spectrum.

The second integral arises from time-varying turbulent fluctuations; its Doppler-broadened spectrum is the subject of the present paper.

IV. SIGNAL CORRELATION

We now proceed to evaluate the second integral in (7). It is convenient at this point to regard the velocity component $u_r(\underset{\sim}{r},t)$ as a random process indexed by the continuous parameters (x,y,z,t), and to redefine the angular brackets in (7) to mean ensemble averaging. This

being done, we assume that the velocity correlation has the following form:

$$\left\langle u_r(\underset{\sim}{r}',t')\, u_r(\underset{\sim}{r}'',t'') \right\rangle = W(\underset{\sim}{r}_{+})\, Q(\underset{\sim}{\xi},\Delta t,\underset{\sim}{r}_{+}) \tag{14}$$

where $\underset{\sim}{\xi}$ is defined in (8), Δt is defined from (10) and (11) by

$$\Delta t = t'' - t' = \tau + (R' - R'')/c \tag{15}$$

and $\underset{\sim}{r}_{+}$ is the centroidal point

$$\underset{\sim}{r}_{+} = \tfrac{1}{2}(\underset{\sim}{r}'' + \underset{\sim}{r}') \tag{16}$$

It is noted that (14) represents a velocity process which is stationary, but not homogeneous (both stationarity and homogeneity, global and local, are understood to be wide-sense properties). The dimensionless weighting function $W(\underset{\sim}{r}_{+})$ is introduced in preparation for an application of Silverman's local homogeneity theory;[2] it will renormalize the space-time correlation to the local value of mean-square fluctuation velocity. The $\underset{\sim}{r}_{+}$ in $Q(\underset{\sim}{\xi},\Delta t,\underset{\sim}{r}_{+})$ arises from our modeling of the frequency spreading due to convection of scattering eddies by a spatially varying mean flow and by macroeddies.

Lighthill[8] and Meecham and Ford[13] have presented arguments showing that the retardation time $(R' - R'')/c$ in (15) can be neglected, and we accordingly shall replace Δt in (14) by the signal lag τ. Changing variables to $\underset{\sim}{\xi}$ and $\underset{\sim}{r}_{+}$, we now denote the second integral in (7) by $F(\underset{\sim}{r},\tau)$ and write

$$F(\underset{\sim}{r},\tau) = 2\pi r^{-2} c^{-5} \rho_o I_i k_o^4 \cos^2\theta \int W(\underset{\sim}{r}_{+})\, Re\left\{ e^{i\omega_o \tau}\, \Phi(\underset{\sim}{k},\tau,\underset{\sim}{r}_{+}) \right\} d^3\underset{\sim}{r}_{+} \tag{17}$$

where *Re* is the real operator, and

$$\Phi(\underset{\sim}{k},\tau,\underset{\sim}{r}_{+}) = (2\pi)^{-3} \int Q(\underset{\sim}{\xi},\tau,\underset{\sim}{r}_{+})\ e^{-i\underset{\sim}{k}\cdot\underset{\sim}{\xi}}\ d^3\underset{\sim}{\xi} \tag{18}$$

In accord with our introduction of local homogeneity assumptions, the integral limits in (17) and (18) are extended to infinity in all directions.[2]

In order for (14) to be a locally homogeneous covariance as defined by Silverman,[2] the weighting function $W(\underset{\sim}{r}_{+})$ must be non-negative and integrable, and $Q(\underset{\sim}{\xi},\tau,\underset{\sim}{r}_{+})$ must be the covariance of a globally homogeneous process. Due to the presence of the $\underset{\sim}{r}_{+}$, representing macroeddy and mean-flow effects, the function Q does not have the required form, however. As noted by Silverman,[3] measurements of Q taken from a system "riding" the macroeddies and mean flow would be essentially devoid of large-scale influences, and the resulting correlation and spectrum would reflect predominantly only the smaller, homogeneous fluctuations. The velocity correlation measured from such a system should have the desired local-homogeneity form, with the variation of Q with $\underset{\sim}{r}_{+}$ strongly suppressed.

Although large-scale velocity variations would be essentially invisible in such a system, the spatially varying mean-square fluctuation level, when normalized to the peak value attained in the vortex, should be the same as that measured in the fixed system. We therefore assume that $W(\underset{\sim}{r}_{+})$ in (14) is the same for either system, fixed or moving.

From Ref. 3 we define the velocity of the moving system at each point $\underset{\sim}{r}_{+}$ to be the space-time average of (2) taken throughout a cube centered

about $\underset{\sim}{r}_+$. The cube must have sides of length much larger than the scattering-eddy size (roughly equal to the incident acoustic wavelength), but smaller than the macroeddy size. Time averaging is over the correlation time of the received scattered signal. We then model the average so obtained by the random process

$$\underset{\sim}{v}_m(\underset{\sim}{r}_+) = \underset{\sim}{u}_o + \underset{\sim}{V}(\underset{\sim}{r}_+) + \underset{\sim}{U}(\underset{\sim}{r}_+) \tag{19}$$

where $\underset{\sim}{u}_o$ and $\underset{\sim}{V}(\underset{\sim}{r}_+)$ are the same nonrandom velocities as before, and $\underset{\sim}{U}(\underset{\sim}{r}_+)$ is a random process governed by some probability law appropriate to the "smoothed-out" macroeddies.

Applying Silverman's results[3] to the present situation (see also Ref. 4), we have the following relationship between the semitransform $\Phi(\underset{\sim}{k},\tau,\underset{\sim}{r}_+)$ in (18), which is measured in the fixed or earth system, and its counterpart $\Phi_m(\underset{\sim}{k},\tau)$ in the moving system:

$$\Phi(\underset{\sim}{k},\tau,\underset{\sim}{r}_+) = \left\langle \exp[-i\,\underset{\sim}{k}\cdot\underset{\sim}{v}_m(\underset{\sim}{r}_+)\,\tau] \right\rangle_o \Phi_m(\underset{\sim}{k},\tau) \tag{20}$$

where the subscripted angular brackets denote ensemble averaging with respect to the probability law of $\underset{\sim}{v}_m(\underset{\sim}{r}_+)$ in (19). We next assume that the vector components of $\underset{\sim}{v}_m(\underset{\sim}{r}_+)$ are jointly Gaussian, with means respectively equal to the components of $\left\langle \underset{\sim}{v}(\underset{\sim}{r},t) \right\rangle$ in (1), and equal standard deviations denoted by $\mu(\underset{\sim}{r}_+)$. Performing the ensemble averaging in (20) then yields

$$\Phi(\underset{\sim}{k},\tau,\underset{\sim}{r}_+) = \Phi_m(\underset{\sim}{k},\tau)\,\exp\{-i\,\underset{\sim}{k}\cdot[\underset{\sim}{u}_o + \underset{\sim}{V}(\underset{\sim}{r}_+)]\,\tau\}\,\exp\{-\tfrac{1}{2}\mu^2(\underset{\sim}{r}_+)\,k^2\,\tau^2\} \tag{21}$$

where k is given by (12). We must now determine suitable functional forms for $\mu(\underset{\sim}{r}_+)$ and $W(\underset{\sim}{r}_+)$.

While measurements of the relatively young vortices generated in wind tunnels have displayed turbulence throughout the entire core,[14] observations of more mature vortices in flight tests indicate a laminar core.[15] This observed absence of inner-core turbulence is consistent with ideas about vortex turbulence advanced by Owen[16] and others. Owen has postulated the existence of a thin annular region at the outer core extremity, i.e., at radius r_c, where turbulent energy production occurs. The radial distribution of turbulence intensity, and hence our weighting function $W(\underset{\sim}{r}_+)$, should therefore peak in this region.

For illustrating the theory, we propose as a qualitative description of the radial variation of turbulence level in a mature aircraft vortex, the square of $f(\sigma)$ in (4). We then include the effect of finite antenna beamwidths in Fig. 1 by truncating the turbulence distribution at $z = \pm L/2$, and write in cylindrical coordinates

$$W(\underset{\sim}{r}_+) = f^2(\sigma)\, g(z) \tag{22}$$

where the gating function $g(z)$ is unity for $|z| < L/2$ and zero otherwise.

Since the macroeddy velocity in a vortex should vary roughly as the mean flow, we adopt for the standard deviation $\mu(\underset{\sim}{r}_+)$ the velocity magnitude from (3),

$$\mu(\underset{\sim}{r}_+) = V_c\, f(\sigma)\, g(z) \tag{23}$$

where $g(z)$ is the same gating function as in (22).

We now wish to replace $\Phi_m(\underset{\sim}{k},\tau)$ in (21) by $\Phi_m(\underset{\sim}{k},0)$. For a spatially uniform macroeddy velocity, an argument given by Ford and Meecham[4] shows that for scattering angles not too near $\theta = 0$ in Fig. 1, the Gaussian

factor in (21) diminishes toward zero in τ much more rapidly than $\Phi_m(\underset{\sim}{k},\tau)$ provided that the macroeddy velocity adequately exceeds the velocities of eddies whose sizes are on the order of the incident acoustic wavelength (i.e., the scattering eddies). In the present situation where the macroeddy velocity $\mu(\underset{\sim}{r}_+)$ is allowed to vary in a manner given by (4) and (23), we assume the incident wavelength to be small enough for this condition to hold over regions of the vortex which contribute heavily to the total scattering — in particular, near the outer-core region.

Noting from (14) and (18) that Φ is calculated from a correlation of r components of velocity, and likewise for Φ_m in (20), we have from Eqs. 3.4.12 and 6.5.3 of Batchelor's monograph on turbulence,[17]

$$\Phi_m(\underset{\sim}{k},0) = [\alpha \varepsilon^{2/3} k^{-11/3} \cos^2(\tfrac{1}{2}\theta)] / (4\pi) \qquad (24)$$

where α is a dimensionless number equal to about 1.4, ε is the dissipation rate of turbulent kinetic energy per unit mass, and k is given by (12). This expression applies to the inertial subrange of incompressible turbulent flows which are also isotropic, and has been cast in terms of the scattering angle θ of Fig. 1.

For evaluating the integral in (17), we shall use the cylindrical coordinates (σ,ϕ,z), with ϕ measured from the positive x axis of Fig. 1 in the direction given by the right-hand rule. In this coordinate system, we shall denote the component of $\underset{\sim}{k}$ in the xy plane of Fig. 1 by k_σ, and shall let ϕ_o be the angle between this xy-plane component and the x axis.

We next regard the mean swirl velocity $\underset{\sim}{V}(\underset{\sim}{r}_+)$ in (19) and (21) as

being in the positive ϕ direction. With the magnitude of $\underset{\sim}{V}(\underset{\sim}{r}_{m+})$ given by (3), the definitions of k_σ and ϕ_o above allow the dot product $\underset{\sim}{k}_m \cdot \underset{\sim}{V}(\underset{\sim}{r}_{m+})$ in (21) to be written

$$\underset{\sim}{k}_m \cdot \underset{\sim}{V}(\underset{\sim}{r}_{m+}) = - k_\sigma V_c f(\sigma) \sin(\phi - \phi_o) \tag{25}$$

We now replace $\Phi_m(\underset{\sim}{k}_m,\tau)$ in (21) by $\Phi_m(\underset{\sim}{k}_m,0)$ in accordance with the discussion above and substitute (21) into (17). Noting from (24) that $\Phi_m(\underset{\sim}{k}_m,0)$ is a real-valued function, we then use (22), (23), and (25) in (17), integrate over z, and write

$$F(\underset{\sim}{r}_m,\tau) = 2\pi L r^{-2} c^{-5} \rho_o I_i k_o^4 \cos^2\theta \; \Phi_m(\underset{\sim}{k}_m,0)$$

$$\times \int_0^{r_o} f^2(\sigma) \exp[-\tfrac{1}{2} V_c^2 f^2(\sigma) k^2 \tau^2] \Lambda(\sigma,\tau) \sigma \, d\sigma \tag{26}$$

where r_o is the overall radius of vortex influence, and

$$\Lambda(\sigma,\tau) = Re\{\exp[i(\omega_o - \underset{\sim}{k}_m \cdot \underset{\sim}{u}_o)\tau] \int_0^{2\pi} \exp[i k_\sigma V_c f(\sigma) \tau \sin(\phi - \phi_o)] \, d\phi \} \tag{27}$$

The integral in (27) has been tabulated (see formula (4.2) of Bowman[18]), and the result is

$$\Lambda(\sigma,\tau) = 2\pi J_o[k_\sigma V_c \tau f(\sigma)] \cos[(\omega_o - \underset{\sim}{k}_m \cdot \underset{\sim}{u}_o)\tau] \tag{28}$$

where J_o is the Bessel function of order zero.

At this point, it is beneficial to make two changes of variables. Since for most functions $f(\sigma)$, the integral in (26) would have to be evaluated numerically, it is convenient to normalize σ and r_o to the core

radius r_c, and to define $\sigma_n = \sigma/r_c$ and $\sigma_o = r_o/r_c$. The second change is to replace the time lag τ by the dimensionless variable ψ defined with the aid of (12) by

$$\psi = kV_c\tau = 2k_o V_c \tau \sin(\tfrac{1}{2}\theta) \tag{29}$$

The signal correlation is best analyzed in terms of the dimensionless ratio $F(\underset{\sim}{r},\tau)/F(\underset{\sim}{r},0)$. To construct this ratio, we use the variables introduced above, and define

$$C(\psi) = [N(\sigma_o)]^{-1} \int_0^{\sigma_o} f^2(\sigma_n) \exp[-\tfrac{1}{2} f^2(\sigma_n)\psi^2] J_o[\psi k_\sigma k^{-1} f(\sigma_n)] \sigma_n d\sigma_n \tag{30}$$

where

$$N(\sigma_o) = \int_0^{\sigma_o} f^2(\sigma_n) \sigma_n d\sigma_n \tag{31}$$

We then insert (28) into (26), multiply and divide by r_c^2 for normalization of σ, and form the ratio $F(\underset{\sim}{r},\tau)/F(\underset{\sim}{r},0)$. In terms of definitions (29) through (31), this ratio can be written

$$F(\underset{\sim}{r},\tau)/F(\underset{\sim}{r},0) = C(\psi) \cos[(\omega_o - \underset{\sim}{k}\cdot\underset{\sim}{u}_o)\tau] \tag{32}$$

The normalized signal correlation thus separates into the product of an envelope function $C(\psi)$ and a cosine.

A plot of $C(\psi)$ for scattering in the *xy* plane of Fig. 1 (where $k_\sigma = k$) appears in Fig. 2. For this plot, numerical integration in (30) was terminated at $\sigma_o = 14$, the value of σ_n at which $f(\sigma_n)$ is down to 0.1. It is noted from (30) that $C(\psi)$ is even in ψ, and the plot is accordingly for positive values of ψ only.

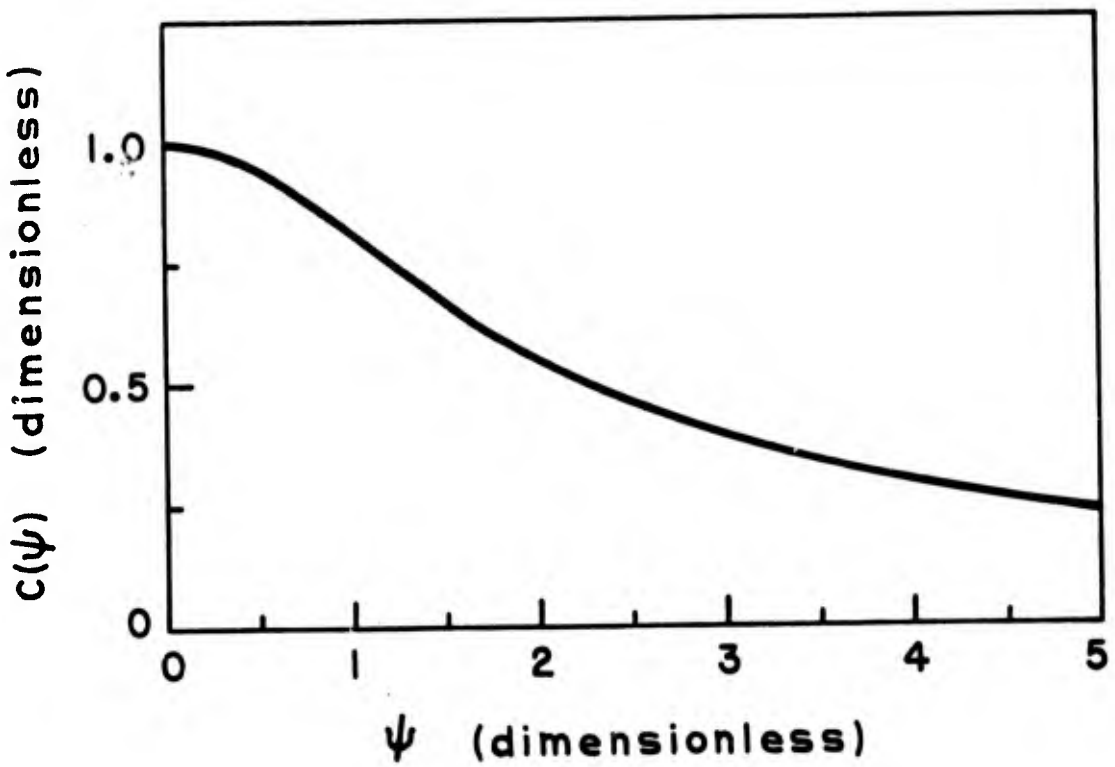

Figure 2. NORMALIZED CORRELATION ENVELOPE FOR SCATTERING IN THE xy PLANE

By replacing k_o in (29) by $2\pi/cT$, where c is the sonic velocity and T the incident wave period, and using the core Mach number defined in (5), we can rearrange (29) to give

$$\tau/T = \psi [4\pi M \sin(\tfrac{1}{2}\theta)]^{-1} \qquad (33)$$

From Fig. 2, $C(\psi)$ is down to 0.5 at $\psi \approx 2.3$. Vortex core Mach numbers for present-day aircraft generally range from about 0.02 to 0.2. For a scattering angle θ of 125 degrees (a local maximum of the scattered intensity, as we shall see), substitution of these numbers into (33) yields a fifty-percent-correlation-level lag of one to ten incident-wave periods, depending on vortex size. In order to utilize inertial-subrange eddies for scattering, the acoustic frequencies employed would range from about 1 to 10 kHz. It is thus seen that the signal correlation time is on the order of milliseconds at most, which is exceedingly small in comparison to time scales of vortex decay for aircraft.

The sonic velocity c, wave period T, and scattering angle θ are easily determined for most experimental setups. Formula (33) then provides a relationship between τ, ψ, and by way of (5), V_c.

Suppose, for example, the lag τ_o at which an experimentally determined correlation envelope is down to a given value is measured. A plot such as Fig. 2 gives the corresponding value ψ_o at which the model envelope is down to this same value. Substituting these values of τ_o and ψ_o into (33), and using (5), then gives the vortex core velocity predicted by the model.

Conversely, given the core velocity of a vortex from which soundings

were taken, the value ψ_o corresponding to a given value τ_o could be obtained from (33). It would then be desirable to have several model curves such as Fig. 2, obtained, say, for different assumed turbulence distributions $W(\underset{\sim}{r}_{\perp})$. A model curve is then sought for which the value $C(\psi_o)$ is equal to the experimental envelope value at lag τ_o, and which matches in overall *form* the experimental envelope. A turbulence distribution for the vortex would thereby be inferred.

These measurements all have analogs in the frequency domain, and we proceed now to derive the power spectral density of the received signal.

V. POWER SPECTRUM

Recalling that $F(\underset{\sim}{r},\tau)$ is the turbulence contribution to the density correlation in (7), we obtain the power spectral density by substituting (26) into (13). Before doing so, however, it is convenient to recast $\Lambda(\sigma,\tau)$ as given by (27) into a slightly different form. To this end, we define

$$\Omega = \omega_o - \underset{\sim}{k}\cdot\underset{\sim}{V}(\underset{\sim}{r}_{\perp}) - \underset{\sim}{k}\cdot\underset{\sim}{u}_o \tag{34}$$

where $\underset{\sim}{k}\cdot\underset{\sim}{V}(\underset{\sim}{r}_{\perp})$ is given by (25). Next, the exponentials in (27) are combined, the real part extracted, and, with the aid of (34), the resulting integrand is written as $\cos(\Omega\tau)$. We then use the Euler formula to express $\cos(\Omega\tau)$ as a sum of complex exponentials, insert this recast version of $\Lambda(\sigma,\tau)$ into (26), then (26) into (13), and write

$$P(\underset{\sim}{r},\omega) = k_o^4 L\,(r\,c)^{-2}\cos^2\theta\;\Phi_m(\underset{\sim}{k},0)\int_0^{r_o}\int_0^{2\pi} f^2(\sigma)\,H(\phi,\sigma,\omega)\;\sigma\;d\phi\;d\sigma \tag{35}$$

where

$$H(\phi,\sigma,\omega) = \tfrac{1}{2}\int_{-\infty}^{\infty} \exp[-\tfrac{1}{2}V_c^2 f^2(\sigma)\, k^2 \tau^2]\left(e^{i\Omega\tau} + e^{-i\Omega\tau}\right) e^{-i\omega\tau}\, d\tau \tag{36}$$

In (36), the complex exponentials can be combined, and with the aid of formula 861.20 of Dwight,[19] the integral is

$$H(\phi,\sigma,\omega) = \frac{(\pi/2)^{\frac{1}{2}}}{k V_c f(\sigma)}\left\{\exp\left[\frac{(\omega-\Omega)^2}{2k^2V_c^2 f^2(\sigma)}\right] + \exp\left[\frac{(\omega+\Omega)^2}{2k^2V_c^2 f^2(\sigma)}\right]\right\} \tag{37}$$

Inserting (37) into (35), it is noted that $P(\underset{\sim}{r},\omega)$ is even in ω. Furthermore, since the velocities $\underset{\sim}{V}(\underset{\sim}{r}_{s+})$ and $\underset{\sim}{u}_o$ appearing in (34) are assumed to be low in Mach number, it is noted from (37) that $P(\underset{\sim}{r},\omega)$ in (35) consists of two spectral pulses which are centered approximately about $\omega = \pm\omega_o$. Since V_c in (37) is likewise a low-Mach-number velocity, the two spectral pulses are distinct, having half-power widths which are a small fraction of ω_o. The two spectral pulses therefore make equal and essentially nonoverlapping contributions to the total scattered intensity as obtained by integrating $P(\underset{\sim}{r},\omega)$ over all values of ω. These arguments show that it is sufficient to examine only one of the pulses in (37), and we arbitrarily elect the one centered at $\omega = \Omega$.

A positive-frequency spectral density could be defined by substituting the desired pulse from (37) into (35). Then, by doubling the result, we would have a spectral function which would still give the total scattered intensity when integrated over ω. We accordingly define

$$P_+(\underset{\sim}{r},\omega) = \frac{k_o^4 L (2\pi)^{\frac{1}{2}}}{k V_c r^2 c^2}\cos^2\theta\ \Phi_m(\underset{\sim}{k},0)\int_0^{r_o}\int_0^{2\pi} f(\sigma)\exp\left[\frac{(\omega-\Omega)^2}{2k^2V_c^2 f^2(\sigma)}\right]\sigma\, d\phi\, d\sigma \tag{38}$$

We now introduce three changes of variables in (38). The first change is from ϕ to $\phi' = (\phi - \phi_o)$. It is noted from (25) and (34) that the resulting integrand in (38) would be periodic in ϕ', and that the limits could therefore be reset to 0 to 2π as before.

The second change is from ω to η, where

$$\eta = [\omega - (\omega_o - \underset{\sim}{k}\cdot\underset{\sim}{u}_o)]/[2\omega_o M \sin(\tfrac{1}{2}\theta)] \tag{39}$$

The variable η is seen to be a normalized deviation from the Doppler-shifted incident frequency. It is noted from (5) and (12) that the denominator in (39) is simply equal to kV_c.

The third change is to multiply and divide (38) by r_c^2 for normalization of the variable σ as before.

We now substitute (25) into (34), the result into (38), make the variable changes listed above, normalize the result to $P_+(\underset{\sim}{r},0)$, and obtain

$$P_n(\eta) = \frac{P_+(\underset{\sim}{r},\eta)}{P_+(\underset{\sim}{r},0)} = \frac{1}{N_+(\sigma_o)} \int_0^{\sigma_o} f(\sigma_n)\, Y(\eta,\sigma_n)\, \sigma_n\, d\sigma_n \tag{40}$$

where

$$Y(\eta,\sigma_n) = \int_0^{2\pi} \exp\{-\tfrac{1}{2}[f(\sigma_n)]^{-2}\, [\eta - k_\sigma k^{-1} f(\sigma_n) \sin\phi']^2\}\, d\phi' \tag{41}$$

and

$$N_+(\sigma_o) = \int_0^{\sigma_o} f(\sigma_n)\, Y(0,\sigma_n)\, \sigma_n\, d\sigma_n \tag{42}$$

A plot of the normalized spectral density $P_n(\eta)$ for the *xy* plane of

Fig. 1 appears in Fig. 3. In this plane, the ratio k_σ/k in (41) is unity. For this plot, the integratiors in both (40) and (41) were performed numerically, with the limit σ_o in (40) set at 14 as done before in (30). It is noted from (40) and (41) that $P_n(\eta)$ is even in η, hence the plot for positive values of η only.

The physical situation is one of small targets — the scattering eddies — being blown around by macroeddies and the mean vortex swirl, and being translated as a group at velocity $\underset{\sim}{u}_o$. The various Doppler effects due to these motions appear in different parts of (40) and (41).

The Doppler shift due to overall translation of the vortex at constant velocity $\underset{\sim}{u}_o$ is manifested by a shift of the center of the spectrum from ω_o to $(\omega_o - \underset{\sim}{k}\cdot\underset{\sim}{u}_o)$. This is seen by noting that since $P_n(\eta)$ is even in η, it is centered about $\eta = 0$. From (39), then, $\eta = 0$ corresponds to $\omega = (\omega_o - \underset{\sim}{k}\cdot\underset{\sim}{u}_o)$. As noted in Section III, the only effect of $\underset{\sim}{u}_o$ taken into account in this solution is the spectral *shifting*. It is assumed that $\underset{\sim}{u}_o$ is small enough for its spectral *broadening* effects to be negligible.

We now wish to obtain a formula for the total 3 dB bandwidth of the received signal. Let us denote by η_c the value of η for which $P_n(\eta) = 0.5$. For this value of η, let the frequency deviation in the numerator of (39) be called $\Delta\omega$. Then (39) can be rearranged to give

$$[2\,\Delta\omega/\omega_o]_{3\text{ dB}} = 4\,\eta_c M \sin(\tfrac{1}{2}\theta) \tag{43}$$

Formula (43) is then an expression for the *total* 3 dB bandwidth of the received signal.

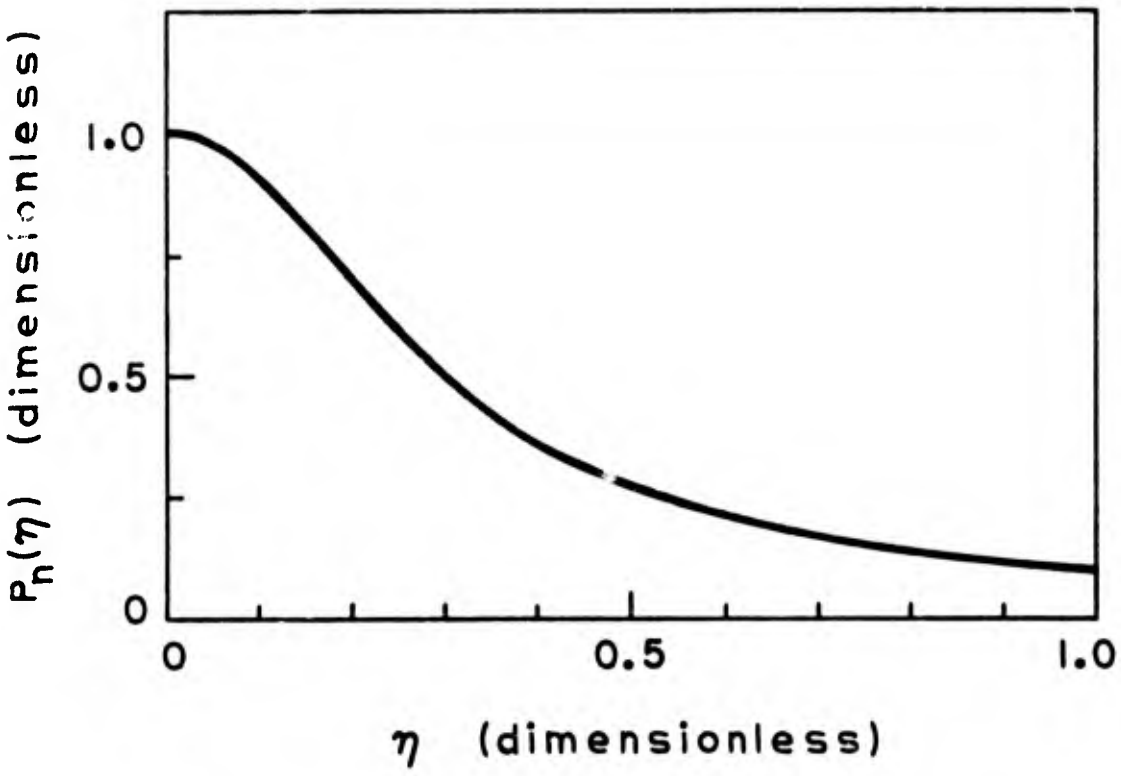

Figure 3. NORMALIZED POWER SPECTRAL DENSITY FOR SCATTERING IN THE xy PLANE.

From Fig. 3, η_c is about 0.3. For a scattering angle θ of 125 degrees, (43) yields a per unit 3 dB bandwidth of about 1.1 M. In other words, the total 3 dB bandwidth of the received scattered signal is expected to be roughly equal to the core Mach number of the vortex.

As a matter of interest, one might inquire as to the relationship between $P_n(\eta)$ in (40) and $C(\psi)$ in (30) and (32). It can be shown that $[(2\pi)^{\frac{1}{2}} N(\sigma_o)\ C(\psi)]$ and $[N_+(\sigma_o)\ P_n(\eta)]$ are Fourier transform pairs.

VI. TOTAL INTENSITY

Rather than integrating one of the spectral density expressions over frequency to obtain the total intensity, it is more convenient to evaluate $F(\underset{\sim}{r},\tau)$ in (26) at $\tau = 0$, and to use the formula

$$I(\underset{\sim}{r}) = c^3\ F(\underset{\sim}{r},0)\ /\ \rho_o \tag{44}$$

Multiplying and dividing (26) by r_c^2 for normalization of σ, setting τ equal to zero, using (12), (24), and (31), and inserting the result into (44), we obtain

$$I(\underset{\sim}{r}) = I_i\, k_o^{\frac{1}{3}}\ (r\,c)^{-2}\, \alpha\, \varepsilon^{\frac{2}{3}}\, \pi\, r_c^2\, L\, N(\sigma_o)\, \cos^2\theta\, \cos^2(\tfrac{1}{2}\theta)\, [2\sin(\tfrac{1}{2}\theta)]^{-11/3} \tag{45}$$

This expression has a local maximum at an angle θ of approximately 125 degrees, the angle which has been used in numerical examples.

The angular pattern in (45) and variation as the cube root of frequency are familiar from the results of previous investigations.[20] In fact, if we were to alter our modeling of the vortex turbulence, and regard the illuminated section in Fig. 1 as a "piece" of a globally

stationary, globally homogeneous velocity process having a spatially and temporally constant mean value, then scattering from the volume of turbulence so defined would fall within the purview of previous analyses.[4,8]

The cylindrical scattering volume, call it V_{sc}, is $\pi r_o^2 L$, or in terms of the normalized radial distance σ_o, is $\pi\sigma_o^2 r_c^2 L$. In the globally homogeneous case, $f^2(\sigma_n)$ in (31) is unity, and $N(\sigma_o)$ is equal to $\frac{1}{2}\sigma_o^2$. Then for this special case, the scattering volume V_{sc} can be written as

$$V_{sc} = 2\pi\, N(\sigma_o)\, r_c^2\, L \tag{46}$$

Using (46), we can write (45) on a per-unit-volume basis as

$$I(\underset{\sim}{r})/V_{sc} = [I_i k_o^2 \cos^2\theta \cot^2(\tfrac{1}{2}\theta)\, E(k)] / (8 c^2 r^2) \tag{47}$$

where, from Batchelor's monograph,[17] $E(k) = \alpha \varepsilon^{2/3} k^{-5/3}$, and k is given by (12). Equation (47) is identical to Eq. 25 of Lighthill's paper,[8] thus providing a check on our results.

VII. CONCLUSIONS

This paper has presented a model for acoustic scattering from a turbulent vortex. The model allows the turbulence intensity, macroeddy velocity, and mean flow velocity to vary with spatial location. Although the functions used in the present paper to describe these spatial variations are in need of experimental confirmation and subsequent improvement, they are adequate for demonstrating the method. The technique should also be useful for analyzing scattering from other turbulent flows where significant variations in turbulence level and mean flow occur over distances on the order of the macroeddy size.

REFERENCES

1. M. Balser, A. E. Nagy, and A. P. Proudian, "Vortex Observations by the Xonics Acoustic Radar at NAFEC," FAA Systems Research & Development Service, Washington, D. C., Rept. No. FAA-RD-71-103, Dec. 1971.

2. R. A. Silverman, Proc. Cambridge Phil. Soc. 54, 530-537 (1958).

3. R. A. Silverman, "Fading of Radio Waves Scattered by Dielectric Turbulence," Courant Institute of Mathematical Sciences, New York Univ., Rept. No. EM-101 (1957).

4. G. W. Ford and W. C. Meecham, J. Acoust. Soc. Am. 32, 1668-1672 (1960).

5. B. W. McCormick, J. L. Tangler, and H. E. Sherrieb, J. Aircraft 5, 260-267 (1968).

6. H. Lamb, *Hydrodynamics* (Cambridge Univ. Press, London, 1932), 6th ed., Chap. 11, pp. 591-592.

7. T. M. Georges, J. Acoust. Soc. Am. 51, 206-209 (1972).

8. M. J. Lighthill, Proc. Cambridge Phil. Soc. 49, 531-551 (1953).

9. L. P. Pitaevskii, Sov. Phys.—JETP 35(8), 888-890 (1959).

REFERENCES (cont'd)

10. E. A. Müller and K. R. Matschat, "The Scattering of Sound by a Single Vortex and by Turbulence," A.F.O.S.R. TN 59-337, AD 213-658, Jan. 1959.

11. A. L. Fetter, Phys. Rev. 136, A1488-A1493 (1964).

12. V. W. Ramsey, "Acoustic Scattering from an Aircraft Trailing Vortex," Ph.D. thesis, Stanford Univ. (1973), Chap. 3.

13. W. C. Meecham and G. W. Ford, J. Acoust. Soc. Am. 30, 318-322 (1958).

14. E. D. Poppleton, J. Aircraft 8, 672-673 (1971).

15. S. C. Crow, Panel discussion in *Aircraft Wake Turbulence and Its Detection*, J. H. Olsen, A. Goldburg, and M. Rogers, Eds. (Plenum Press, New York, 1971), pp. 577-583.

16. P. R. Owen, Aeron. Quart. 21, 69-78 (1970).

17. G. K. Batchelor, *Homogeneous Turbulence* (Cambridge Univ. Press, London, 1956), pp. 49 and 122.

18. F. Bowman, *Introduction to Bessel Functions* (Dover, New York, 1958), P. 57.

REFERENCES (cont'd)

19. H. B. Dwight, *Tables of Integrals and Other Mathematical Data* (MacMillan, New York, 1961), p. 236.

20. C. G. Little, Proc. IEEE 57, 571-578 (1969).